6-2019

Statistical optimization of stress level in Mg-Li-Al alloys upon hot compression testing

Rezawana Islam

Meysem Haghshenas
University of North Dakota, meysam.haghshenas@UND.edu

Available online at www.sciencedirect.com

ScienceDirect

Journal of Magnesium and Alloys 7 (2019) 203–217

www.elsevier.com/locate/jma

Full Length Article

Statistical optimization of stress level in Mg-Li-Al alloys upon hot compression testing

Rezawana Islam, Meysam Haghshenas*

Department of Mechanical Engineering, University of North Dakota, Grand Forks, ND, USA

Received 17 December 2018; received in revised form 25 March 2019; accepted 31 March 2019
Available online 13 May 2019

Abstract

In the present study, a response optimization method using Extreme Vertices Mixer Design (EVMD) approach is proposed for stress optimization in a thermomechanically processed Mg-Li-Al alloy. Experimentation was planned as per mixed design proportions of Mg, Li and Al and process variables (i.e. temperature and strain rate). Each experiment has been performed under different conditions of factors proportions and process variables. The response, particularly stress has been considered for each experiment. The response is optimized to find an optimum condition when the contributing factors influence material characteristics in such a way, to achieve better strength, ductility and corrosion resistance. Estimated regression coefficient table for response has been observed to identify the important factors in this process and significantly high variance inflation factor has been observed. Most importantly, an optimum condition is achieved from this analysis which fulfills the experimental observations and theoretical assumptions.

Keywords: Mg-Li-Al alloy; Design of experiments (DOE); Extreme vertices mixture design (EVMD); Stress optimization.

1. Introduction

Magnesium alloys possess growing demands due to their relatively high specific strength and low density in the transportation and automobile industries [1,2]. Due to hexagonal close-packed (hcp) crystalline structure and therefore limited slip system, deformation behavior of pure Mg at room is very limited [3–5]. To this end, the addition of Li to Mg increases ductility without sacrificing the total density of the Mg-Li alloy [6,7] which make them unique for many weight-saving applications.

The Mg-Li phase diagram (Fig. 1) shows that Li is soluble in hcp α-phase up to 4 wt% producing a high strength family of Mg-Li alloys. However, Mg alloyed with greater than 12 wt% Li has a bcc structure (β-phase) [8,9]; this family of the alloys shows more ductility, therefore less stress is required to deform at different temperatures and strain rates. Ductility of the hcp α-phase is less than the bcc β-phase of Mg-Li alloys. Disadvantages of Mg-Li alloys with bcc structure include a high chemical activity and poor corrosion resistivity [10]. Because Li is highly reactive. As a result for the applications where the strength of the material is the highest priority, hcp structured α-Mg phase is preferred, as this type of structure ensures good strength materials for practical application [11] but does not possess good ductility.

Though the Mg-Li-Al alloys have comparatively low density and good formability, due to inferior corrosion resistance, rapid development and application of this kind of alloy is getting limited. In general, there are multiple influential factors that reduce the corrosion resistance of Mg-Li-AL alloys; microstructure, the chemical composition, application environment and surface treatment. Therefore, utilizing alloying, heat treatment and plastic deformation techniques are promising approaches to enhance the corrosion resistance of the alloys. Also, the addition of Al into Mg-Li alloys can make better the corrosion resistance of Mg-Li alloys [12].

* Corresponding author.
E-mail addresses: meysam.haghshenas@engr.und.edu, mhaghshe@alumni.uwo.ca (M. Haghshenas).

https://doi.org/10.1016/j.jma.2019.03.003

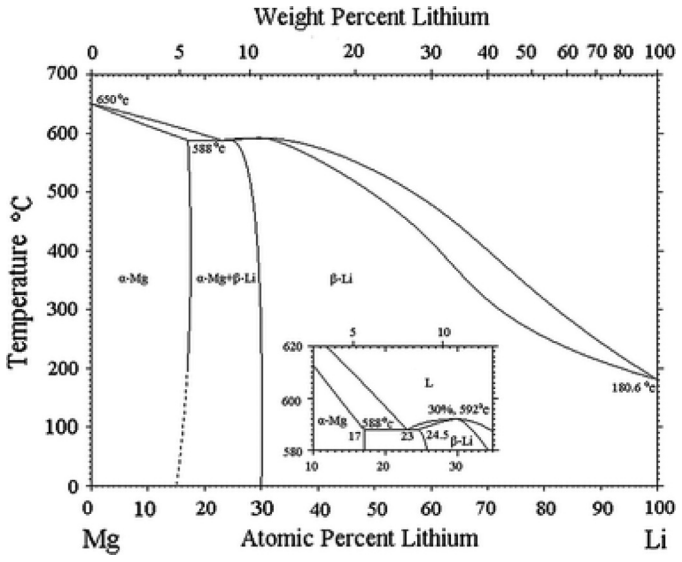

Fig. 1. Mg-Li phase diagram [18].

Aluminum addition in Mg-Li increases the c/a ratio. In a study by Haferkamp et al. [13] it was estimated that Al content considerably increases the yield stress, maximum stress and ductility at room temperature [13]. Both, Zn and Al possess good solubility in Mg-Li alloy. Al can be dissolved in solid solution in a well manner. When Al contents reached up to 3 wt% in Mg-Li solid solution, Al-Li compound is formed. Most importantly, the accurate inclusion of Al may increase the strength without deterioration of density. Zn has similar kind of effects in comparison to Al inclusion, but density goes up (7.133 g/cm3). Therefore, Al (2.7 g/cm3) accounted as a proper additional element to keep the advantage of being lightweight and also to strengthen the alloy by means of grain size refining, solid solution hardening, and compound reinforcements. As a result, Mg-Li-Al alloys are having an excellent lightweight characteristics and mechanical properties [14]. Also, thermomechanical processing (TMP) helps improve the corrosion resistance ductility and formability of this alloy. Plastic deformation at elevated temperature. It is common technique utilized to improve the mechanical properties of Mg alloys. Especially in case of Mg-Li alloys TMP has a huge impact to change and develop the mechanical properties [15]. Hot deformation of metallic materials which includes work hardening, dynamic recovery and dynamic recrystallization, can prompt changes in the microstructure of the deformed material which are specifically reflected in the flow stress curves. The effect of TMP in Mg-Li alloys. Cold working increases the hardness, strength but reduce the ductility along with grain size. Due to increase in temperature annealing starts and releases the internal stress resulting in dynamic recovery. Hot working involves deformation at temperatures where recrystallization can occur and flow stress goes down, improves ductility but reduces strength and hardness.

Therefore, identification of the accurate blending of the alloying elements and process variables can be lengthy and costly during the experimentation. Design of experiment is such a branch of applied statistics deals with planning, conducting, analyzing, and interpreting controlled tests to evaluate the factors that are important in various analysis.

In a study by Wangkananon et al. [16] the EVMD approach is taken to optimize inhibition effects and also to make the assumptions for further experimentation. In another study, by

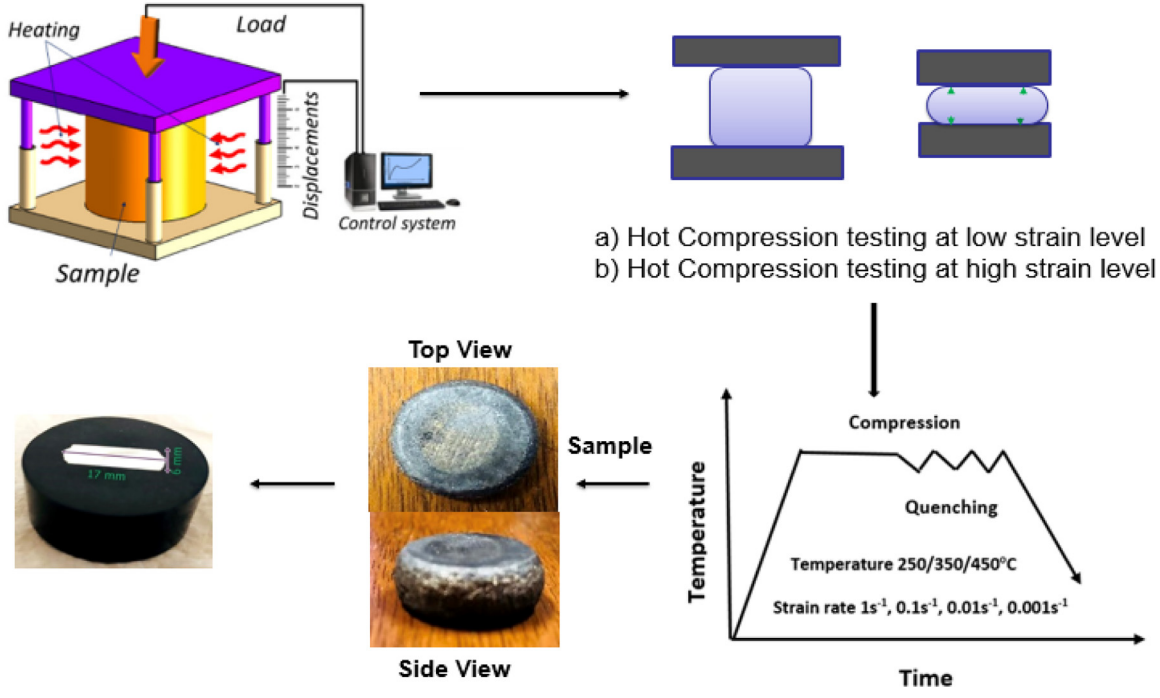

Fig. 2. Schematic of the experimental setup.

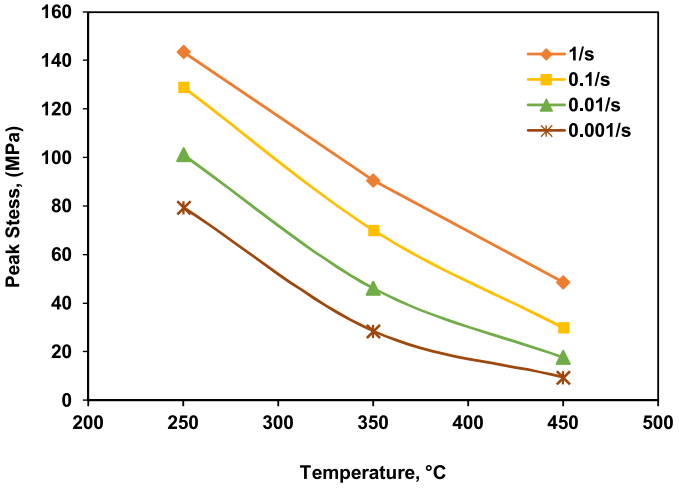

a

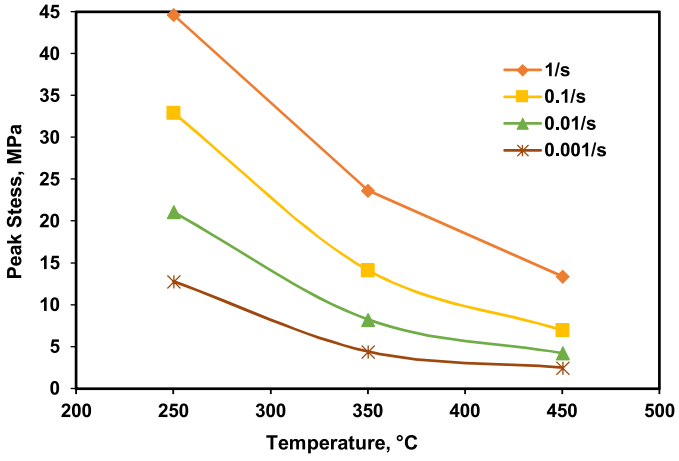

b

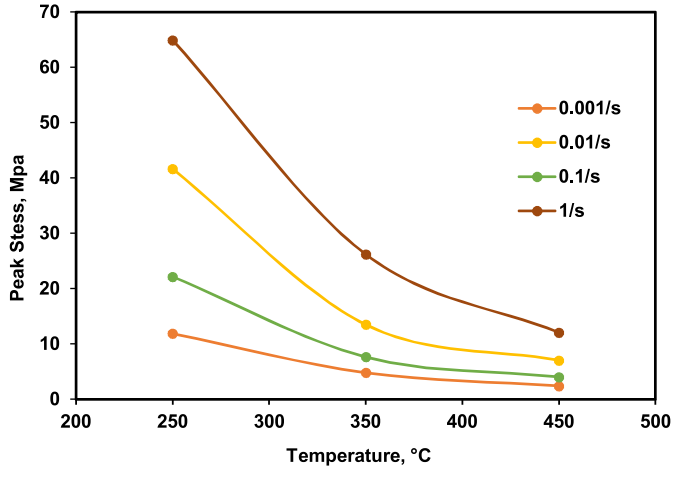

c

Fig. 3. Peak stress for (a) Mg −3.5 wt%-Li-Al alloy, (b) Mg −8.5 Li%-Al alloy, (c) Mg −14 wt%-Li-Al alloy.

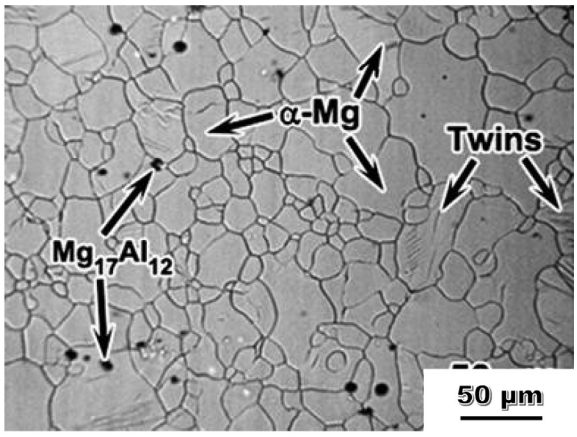

a

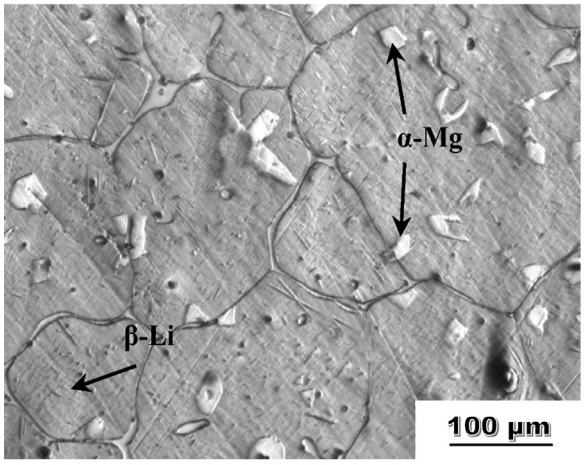

b

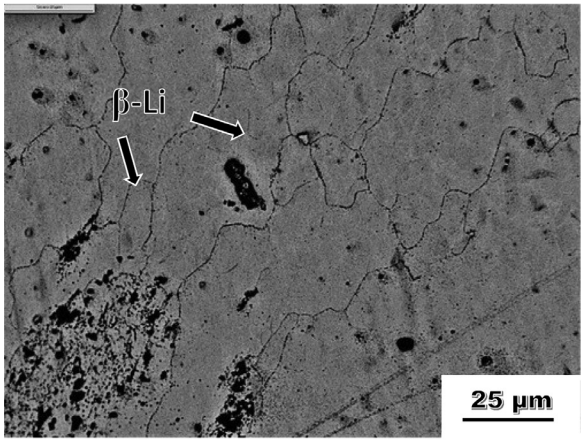

c

Fig. 4. Microstructural observations (a) single α-phase [27] (b) dual (α + β) phase [28] (c) single β-phase Mg-Li-Al alloy.

Richmire et al. [17], Taguchi method was employed to significantly reduce the number of required experiments and identify the statistical significance in friction stir welded AM60 Mg alloys. Glajch et al. [18] used an interactive mixture-design statistical technique to optimize solvent strength and selectivity for reversed-phase liquid chromatography.

Table 1
Upper and lower constraint table for mixer design.

Components & process variables	Upper boundary	Lower boundary
Mg	0.945	0.86
Li	0.14	0.035
Al	0.015	0.01
Temperature	450 °C	250 °C
Strain rate	1/s	0.001/s

Table 2
Analysis of variance for component proportions (Minitab analysis).

Source	DF	Seq SS	Adj SS	Adj MS	*F*-Value	*P*-Value
Regression	17	113,027	113,027	6648.67	159.83	0.000
Component only						
Linear	2	31,940	5662	2830.94	68.05	0.000
Quadratic	3	6792	6792	2264.06	54.43	0.000
Mg*Li	1	6746	5331	5331.41	128.16	0.000
Mg*Al	1	36	10	9.64	0.23	0.631
Li*Al	1	11	11	10.84	0.26	0.611
Component * Temp						
Linear	3	47,265	3235	1078.42	25.92	0.000
Mg*Temp	1	35,989	430	430.39	10.35	0.002
Li*Temp	1	11,251	1377	1377.13	33.10	0.000
Al*Temp	1	25	40	40.14	0.96	0.329
Quadratic	3	2356	2356	785.21	18.88	0.000
Mg*Li*Temp	1	2305	1489	1489.39	35.80	0.000
Mg*Al*Temp	1	11	40	40.46	0.97	0.327
Li*Al*Temp	1	39	39	39.19	0.94	0.335
Component * Strain rate						
Linear	3	23,147	1783	594.30	14.29	0.000
Mg*Strain rate	1	21,984	347	346.53	8.33	0.005
Li*Strain rate	1	1161	808	807.67	19.42	0.000
Al*Strain rate	1	3	96	95.64	2.30	0.133
Quadratic	3	1528	1528	509.21	12.24	0.000
Mg*Li*Strain rate	1	1428	781	781.32	18.78	0.000
Mg*Al*Strain rate	1	5	96	95.93	2.31	0.133
Li*Al*Strain rate	1	95	95	94.67	2.28	0.135
Residual Error	82	3411	3411	41.60		
Lack-of-Fit	34	3390	3390	99.71	228.49	0.000
Pure Error	48	21	21	0.44		
Total	99	116,438				

The aim of this paper is to statistically optimize the response (flow stress) of a Mg-Li-Al alloy when changing the Mg, Li, and Al proportions and to process the variables (temperature and strain rate) using the EVMD analysis. To find the optimal level of the proportions when the mechanical properties are satisfactory, optimization is done and multi-linearity is observed as a result of the regression analysis.

In the present study, to manipulate the data, Minitab 18 is used through the EVMD which is an orderly method to design with the presence of both lower and upper bound constraints on the components. Here, the response is a function of the proportions of every components or factor in the mixture. In mixture-process variable design, the response is very much likely to depend on the proportion of the factors and process variables which are factors as well but not included in the mixture [19]. This method could significantly reduce the number of required experiments and statistical

Table 3
Estimated regression coefficients for stress.

Term	Coef	SE Coef	*T*-value	*P*-value	VIF
Mg	162.06	7.65	*	*	110.79
Li	6976	589	*	*	7555.13
Al	−1188	363	*	*	49.28
Mg*Li	−9084	722	−12.59	0.000	8692.01
Mg*Temp	−84.42	5.32	−15.88	0.000	53.54
Li*Temp	−3858	580	−6.65	0.000	7338.84
Mg*Li*Temp	5080	712	7.14	0.000	8460.87
Mg*Strain rate	53.69	5.32	10.10	0.000	53.54
Li*Strain rate	3201	580	5.52	0.000	7338.84
Mg*Li*Strain rate	−4040	712	−5.67	0.000	8460.87

significance of the parameters can be identified to optimize the response. An optimization is an important tool in design analysis where controllable factors can be set to a certain point so that the robustness of the design or process gets improved.

2. Experimental procedure

Thermomechanical processing (TMP) is a mechanical deformation technique by shaping and heating operations which has been employed toward deformation of Mg-Li alloys so far [20–22]. Usually performed at high temperatures and different strain rates affecting the stress level. The TMP samples used in this study were machined out of the as-received Mg-Li-Al extruded alloy. Small solid cylinders, hot compression (thermomechanical) cylinders with an aspect ratio of 1.5 (length: 15 mm and diameter: 10 mm), were cut in the extrusion direction. Using a Gleeble® 3500 thermal-mechanical simulation testing system, the samples were isothermally compressed at temperatures of 250 °C, 350 °C and 450 °C and different strain rates of 0.001 s^{-1}, 0.01 s^{-1}, 0.1 s^{-1}, and 1 s^{-1}. Upon completion of each test, the specimens were quenched as soon as possible to freeze the deformed microstructure. During testing, stress-strain curves were recorded online using a computerized system attached to the compression system. Schematic of the experimental setup is provided in Fig. 2.

3. Microstructures and properties analysis

3.1. Flow graphs

The consecutive results from the experimentation of this analysis during hot compression are presented in flow graphs, which can illustrate the variations in stress levels clearly. At a constant temperature, when the strain rate increases, flow stress enhances. By the same token, when the strain rate is constant, by increasing the temperature, the flow stress decreases. The response optimization depicts the exact stress level at different temperatures from 250 °C to 450 °C and different strain rates from 0.001/s to 1/s for Mg-3.5 wt%-Li alloy from experimental analysis. The peak stresses from Fig. 3a

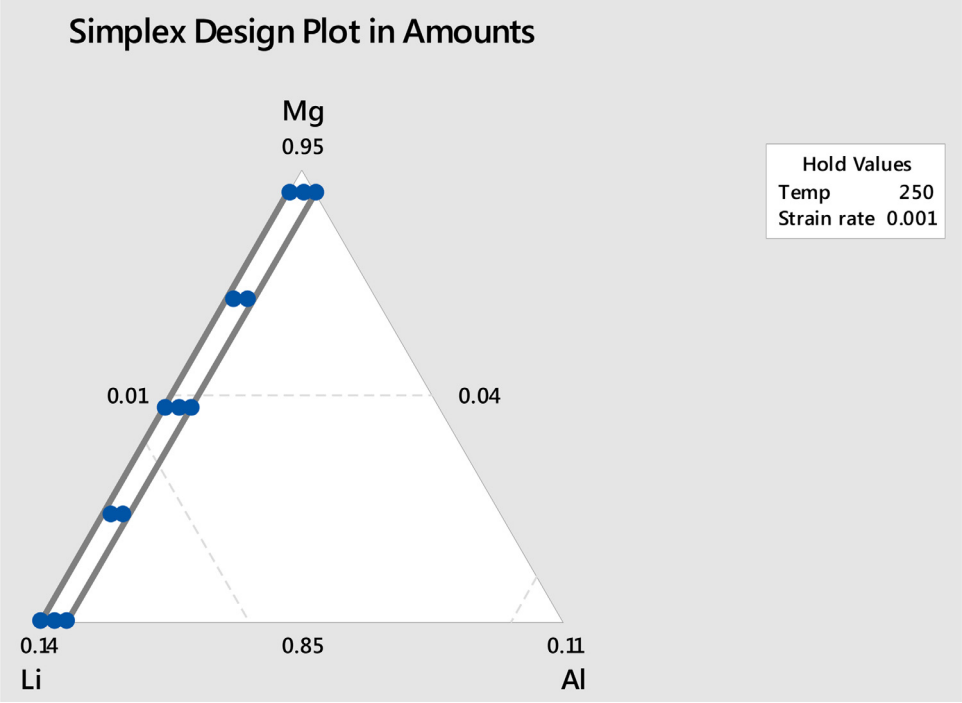

Fig. 5. Simplex design plot.

found for the alloy at 250 °C for the four different strain rates are 143.5 MPa, 129.4 MPa, 101.8 MPa and 79.3 MPa which is comparatively higher than others.

When Li percentage is below 5 wt%, the alloy possesses completely hcp structure. The addition of Li to Mg increases the critical resolved shear stress (CRSS) for basal slip and a solid solution hardening is observed. The CRSS of this alloy is almost independent of the temperature above room temperature while the CRSS for non-basal slip decreases with increasing temperature. The addition of Li results in a decrease in both a and c lattice parameters in the Mg-Li solid solution [23]. Also, the addition of Al in this alloy creates Al-Li precipitates which affects not only the yield stress but also the storage of the dislocations during plastic deformation [23], thus, increasing strength. Both solid solution and precipitation hardening in the structure would increase the strength. Because of high strength during deformation through thermo-mechanical processing (TMP), higher stress is recorded.

The scenario is quite different in the case of Li more than 12 wt% in Mg; Fig. 3b shows that peak stresses are comparatively lower than the stress shown in Fig. 3a for different temperatures and strain rates; though the temperature and strain rate have similar effects on both type of alloys. Basically, due to the addition of Li more than 12 wt%, this type of alloy possesses more active slip systems, hence better ductility; however, the strength is compromised which is not beneficial for structural applications.

If stress can be optimized, it is possible to find an accurate blend of Mg, Li and Al holding the required temperature and strain rate when strength and ductility need not to be compromised. At the same time, better corrosion resistance is achievable.

Fig. 3c shows such a combination where both strength and ductility is achievable. In dual phase alloy, at 250 °C the peaks for stress is fairly high in comparison to the 350 °C–450 °C specially at higher strain rate. That level of peak stress variation has not been observed at single phased alloys.

After thermomechnaical processing both α and β phases add to the deformation mechanism. In α phase, there exists certain amount of dislocations but that amount is very low for β phase. This might be identified as the difference in the recovery and dynamic recrystallization between α and β phases during TMP at elevated temp. It was accounted that the stacking fault energy (SFE) plays a improtant role in controlling the event of dynamic recovery and recrystallization. A high SFE is valuable to the dynamic recovery and recrystallization amid thermo-mechanical processes. Therefore, dislocation annihilation happens throughout the dynamic recovery and recrystallization process in the bcc β phase, the one with a higher stacking fault energy; on contrary the SFE of α phase is lower, impeding the event of dynamic recovery and recrystallization. Therefore, large amount of dislocations can be stayed in grains of α phase or just be around α/β interfaces and strength increased.

The penchant to twin is controlled due to the expanded SFE with Li increments. It is very much acknowledged that inclusion of Li in Mg alloy enhances the stacking fault energy (SFE), which advances cross-slip and climb of dislocations of non-basal slips. Thus, better ductility at β-phase is achieved.

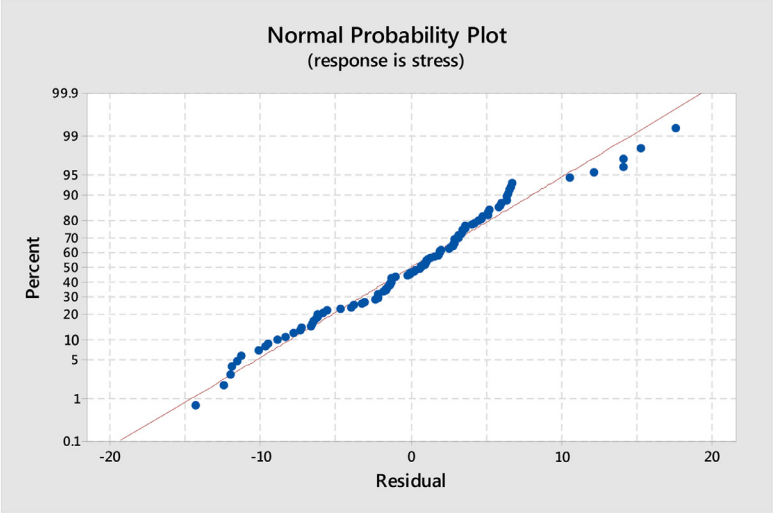

a

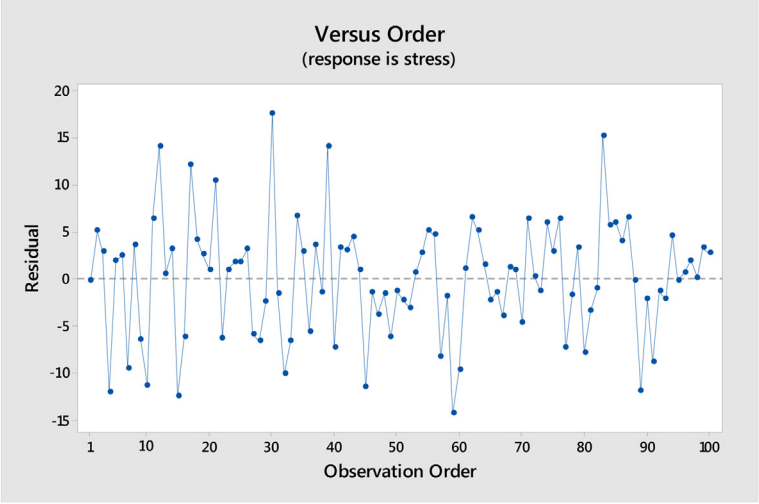

b

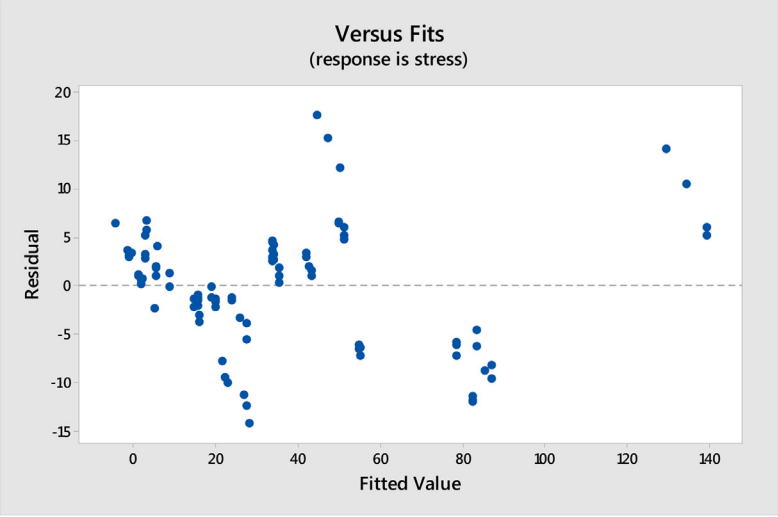

c

Fig. 6. (a) Normal plot for residuals, (b) Versus order plot for residuals, (c) Versus fits plot for residuals.

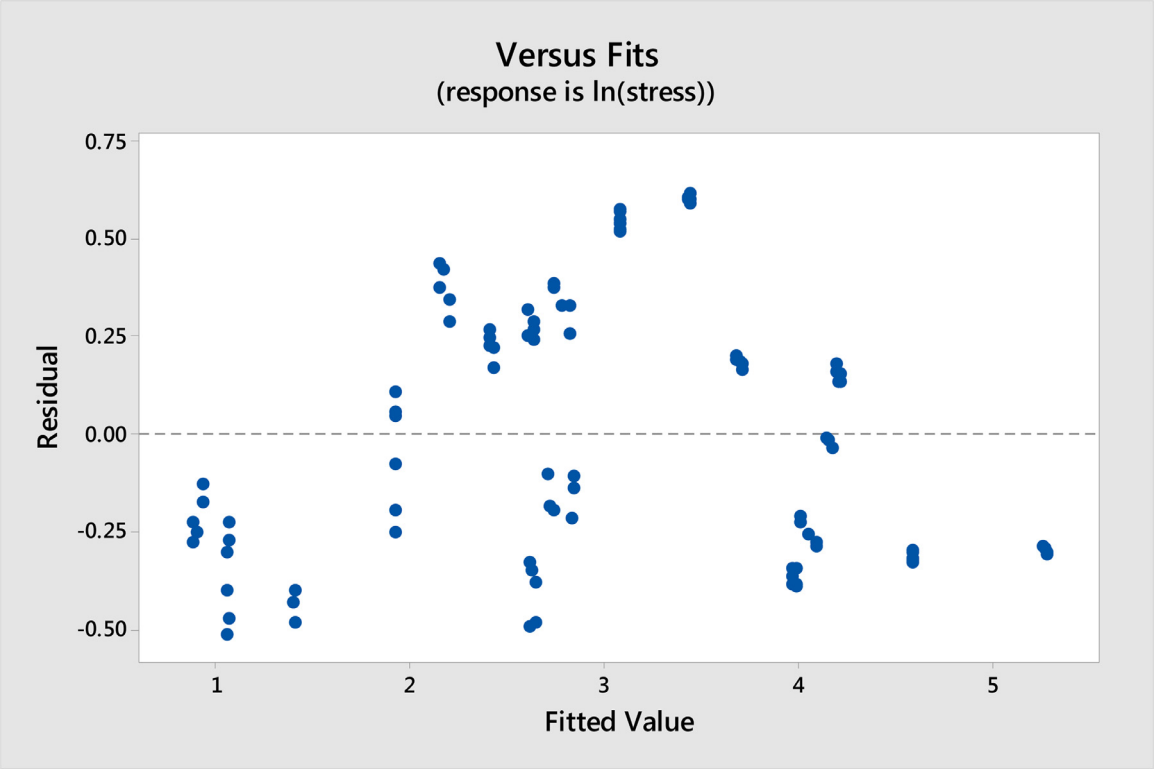

Fig. 7. Versus fits plot after data transformation.

3.2. Microstructural observations

Fig. 4a illustrates that the α–Mg phase has some twins and $Mg_{17}Al_{12}$ precipitates which aids to improve the strength of this stage. Also, Al solubility in Mg compare to Li is very high and helps in strengthening the phase [24] using solution strengthening mechanism. But this type of alloy lacks ductility.

The microstructure below (Fig. 4b) showed a duplex phase microstructure which includes β-Li matrix and distributed α-Mg phases having a shape like petal in Mg with 9wt%Li alloy. (Figure) [12]. Here, α-Mg phase demonstrated coarsened grains which means that the alloy had to go through dynamic recrystallization around 350 °C. And more number of dislocations generated in β-Li phase as a result plastic deformation is more in this zone. Li increases the plasticity of Mg [24]. Thus, both the harder and softer phases co-exist. These act like a balanced combination of strength and ductility.

Also, it has been observed (Fig. 4c) that in Mg with 14wt%Li alloy β grains are elongated and as a result this alloy possesses comparatively high ductility even at low strain rates but strength is reduced.

4. Design steps in Minitab

4.1. Design components

The Mg-Li-Al alloy, assessed in the present study, possesses three design components or factors needed to analyze to optimize the stress as a response.

4.2. Process variables

Temperature and strain rate are experimental factors, though these are not part of the mixture but has an effect on the response of the design.

4.3. Upper and lower bounds

Constrained designs (one with upper and lower boundary) create coefficients that are highly correlated. If the lower bound of the design is changed of one component, the upper values change as a result. Minitab calculates like this:

Ui = Total for mixture - [L1+L2+...+ L(i-1)+L(i+1)+...+Lq] where L is the lower bound and q is the number of components [25].

The components and the process variables in this design contain the following upper and lower boundaries:

4.4. Extreme vertices design

Extreme vertices designs are mixture designs that cover only a subportion or smaller space within the simplex. These designs must be used when chosen design space is not a L-simplex design (see Fig. 4). The presence of both lower and upper bound constraints on the components often create this condition. For this particular design, three components and two process variables with lattice degree two, there are 100 design points. Process variables (no replication) included as full factorial design. Mixture total is 1. Therefore, the sum of the components is equal to 1 [26].

4.5. Augmented design

The design has been augmented with one center point and three axial points. To adequately cover the response surface we need a design with interior points. Each of additional points is a complete mixture as well.

5. Response

Stress is acting as a response in this design analysis. For each sum of the components in the design, we put stress as response collected from the experimental analysis during the TMP of the Mg-Li-Al alloy.

6. Results and analysis

6.1. Simplex design plot

There are 13 points in the design space. The proportions of the components are selected for each point in such a manner that they sum to one. The solid grey contour represents the design space for this mixture design. Table 1

6.2. Data interpretation

From Table 2 it is observed that some factors where *P* values are considerably higher than significant 0.05. Therefore, the reduced model is formed and the number of experiments reduced to remove the non-significant factors. From the analysis of variance table, it is confirmed that Al is a nonsignificant factor in this design.

6.2.1. Reduced model

Key results from the effect of regression coefficient analysis are presented in Table 3.

6.2.2. P-Value

From the above analysis we have observed that all the *P* values are less than significant level of 0.05 and it is almost 0.000 for the main effects and interactions as well. Therefore, it is obvious that the association is statistically significant. All these factors and their interaction effects are significant.

6.2.3. Coefficients

We have observed some negative coefficient values during the interaction of Mg & Li, Mg & Temperature, Li & Temperature, Mg, Li & strain rate. For all these terms mean stress value is less than the value can be obtained by simple hand calculation for each pure mixture. Interactions with positive coefficients greater mean stress value than the value obtained by simple calculation for each pure mixture.

6.2.4. R-sq value

R-sq value is 96.71%, therefore the mixture model fits data quite well. Also, R-sq (Predicted) value shows that the model is not over-fit.

6.3. Residual plot analysis

The normal probability plot (Fig. 5a) for residual shows that data set follows the fitted distribution line. Most of the points fall closely along the center line, there are few outliers. Therefore, the residuals are normally distributed. The residuals versus order (Fig. 5b) plot fall randomly around center line without following any particular type of pattern. Therefore, the residuals are independent of one another.

The residuals versus fit plot (Fig. 5c) exhibits that data are not well scattered. Still, we can see some vacant space. As a matter of fact, natural log data transformation has been employed.

6.4. Data transformation

To analyze variability in response data for experiments with replicated measurements data transformation is used. Particularly, natural log is used in this statistical analysis to improve the probability density functions for many distributions.

After data transformation (Fig. 6) the scale of the newly fitted values changed and we achieved a good fit in the residual versus fits plot; it has well-distributed density function improving the variance constancy.

6.5. Main effect plot

From the analysis of variance for stress, we observed that the main effects are Mg, Li proportions, Temperature, Strain rate, and their interactions. From the interaction plot for process variables (Fig. 7a), we see that with the increase of temperature stress goes down and with an increase of strain rate stress goes up. Also, with increasing the proportion of Mg the stress value rises and reducing the Li proportion the stress goes up (Fig. 7b).

6.6. Interaction plot

Interaction plot (Fig. 8) demonstrate the same type of results. For a constant temperature, high strain rate gives high stress and low strain rate yields low stress. Also, considering the constant strain rate, low temperature increases the stress and high temperature decreases the stress level.

6.7. Surface plot

For the surface plot, the temperature is held constant at 250 °C and the strain rate at 0.001/s. The surface plot (Fig. 9)

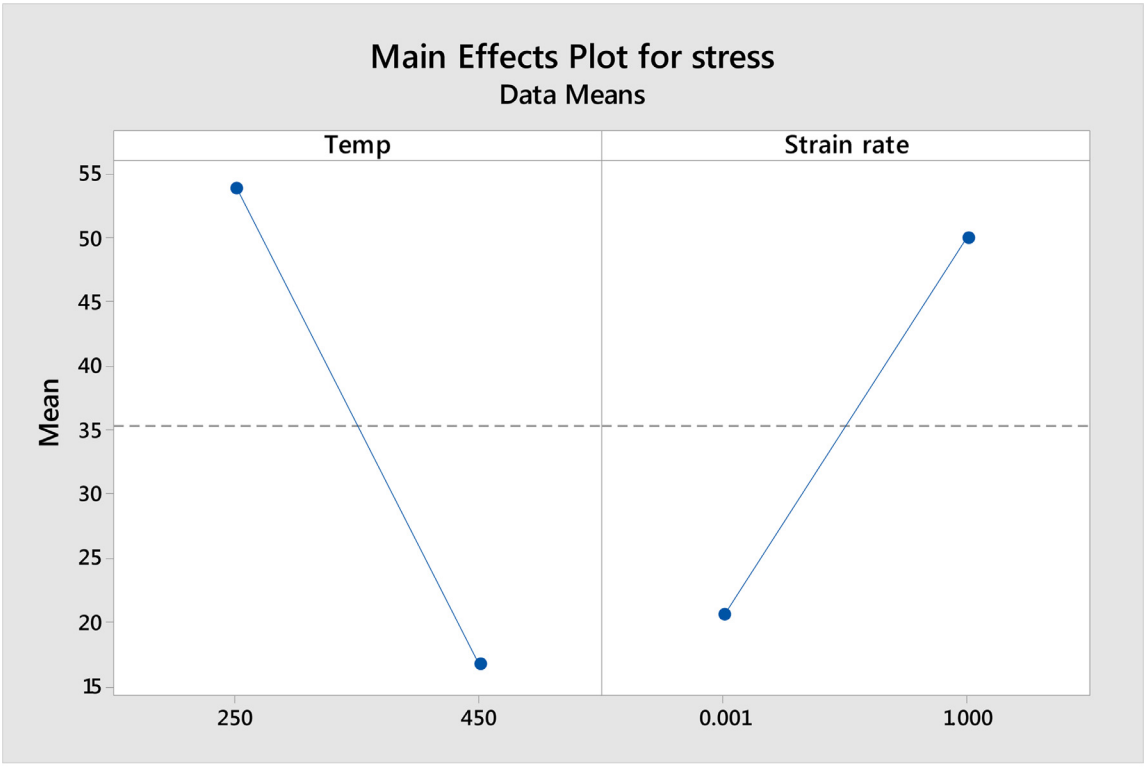

a

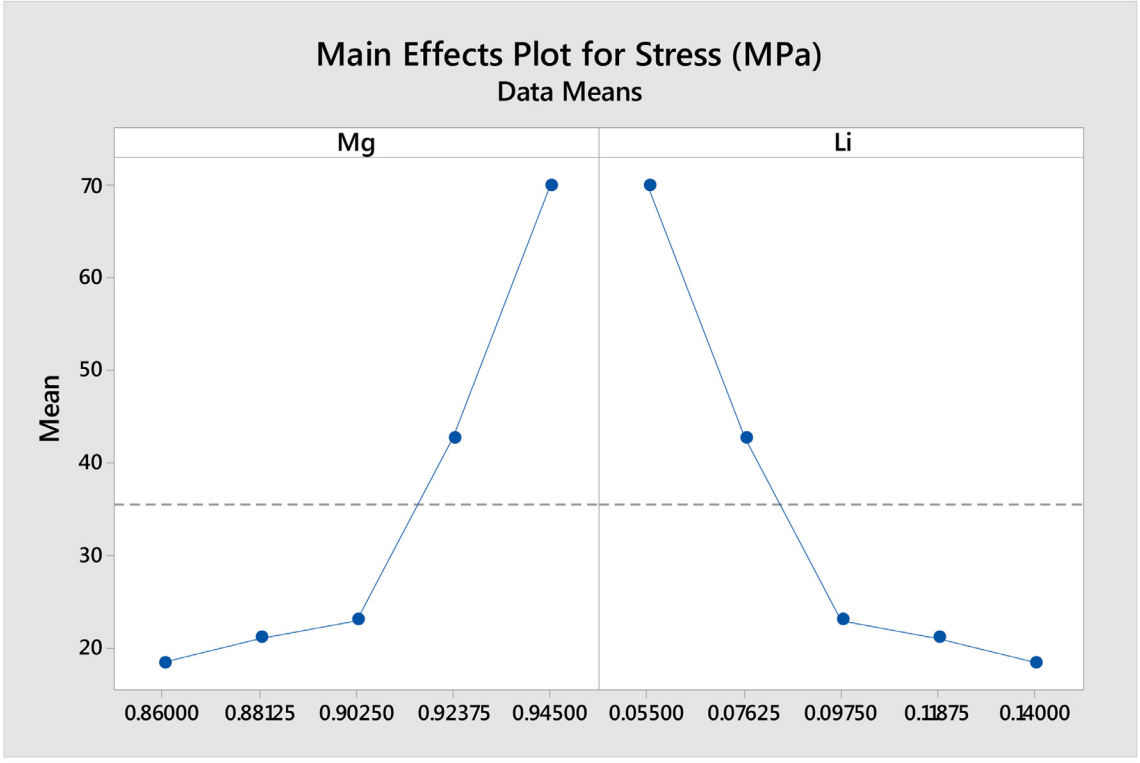

b

Fig. 8. Main effect plot for (a) process variables, (b) factors.

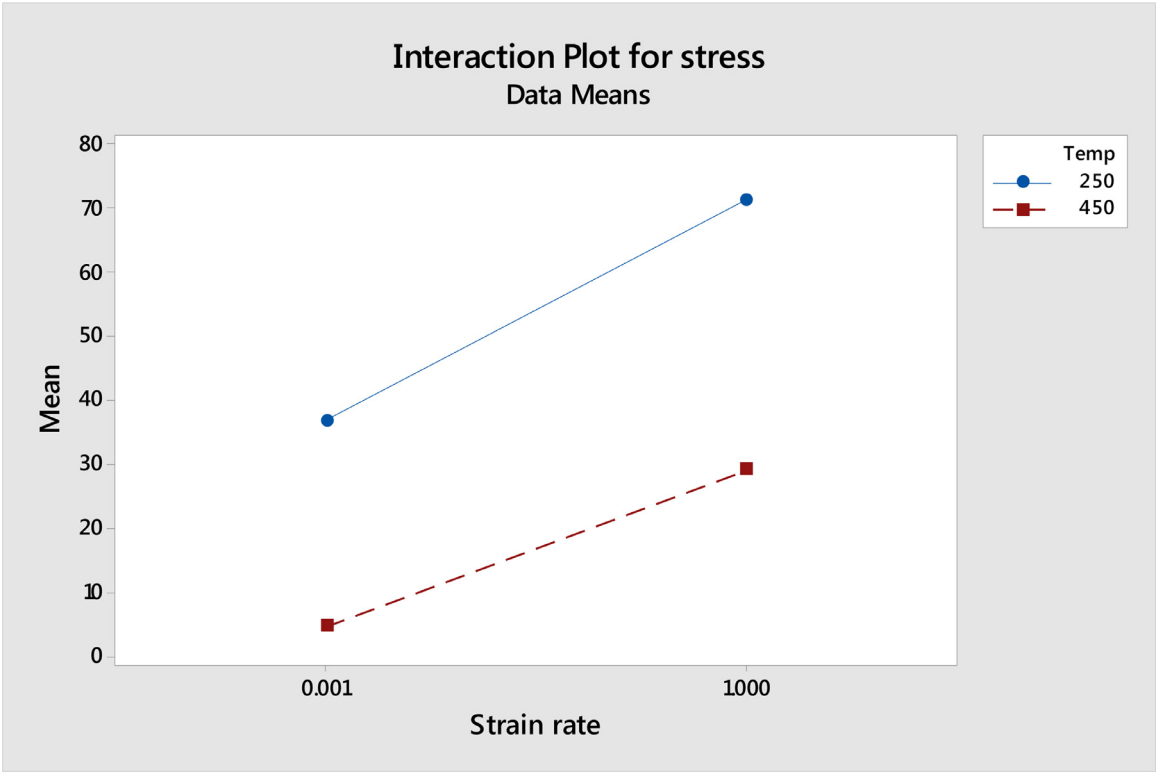

Fig. 9. Interaction plot for a response.

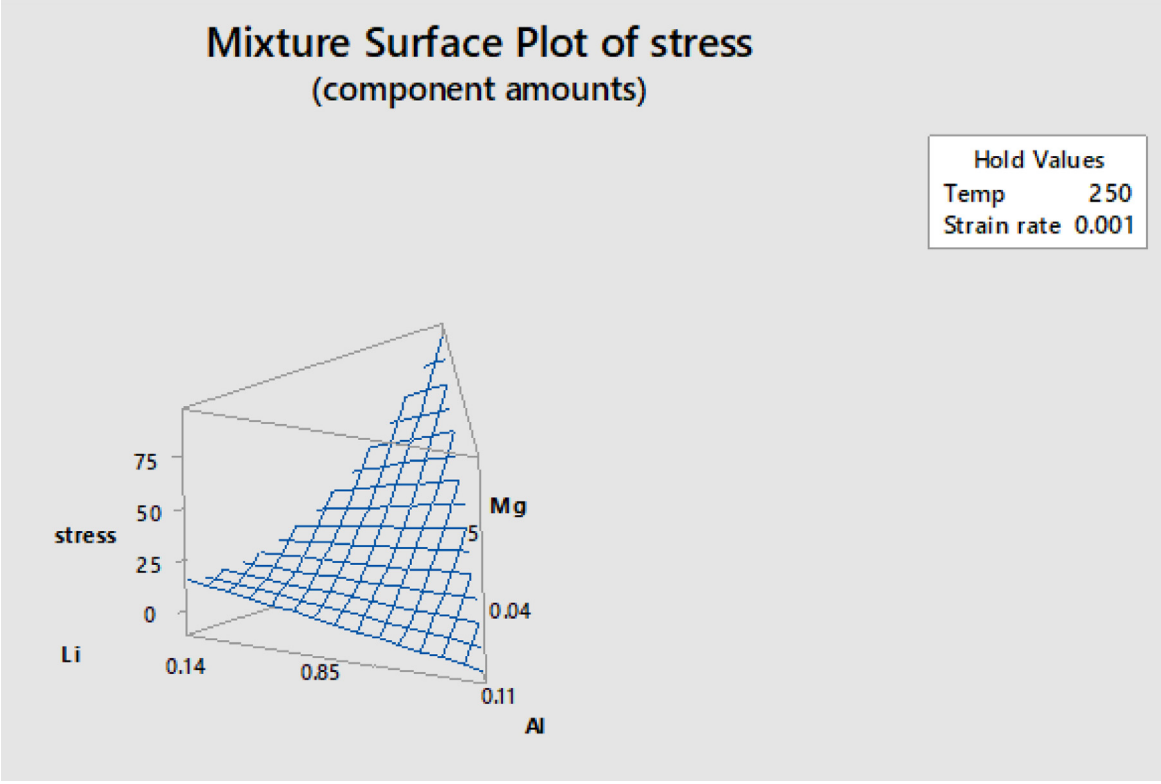

Fig. 10. Surface plot for a response.

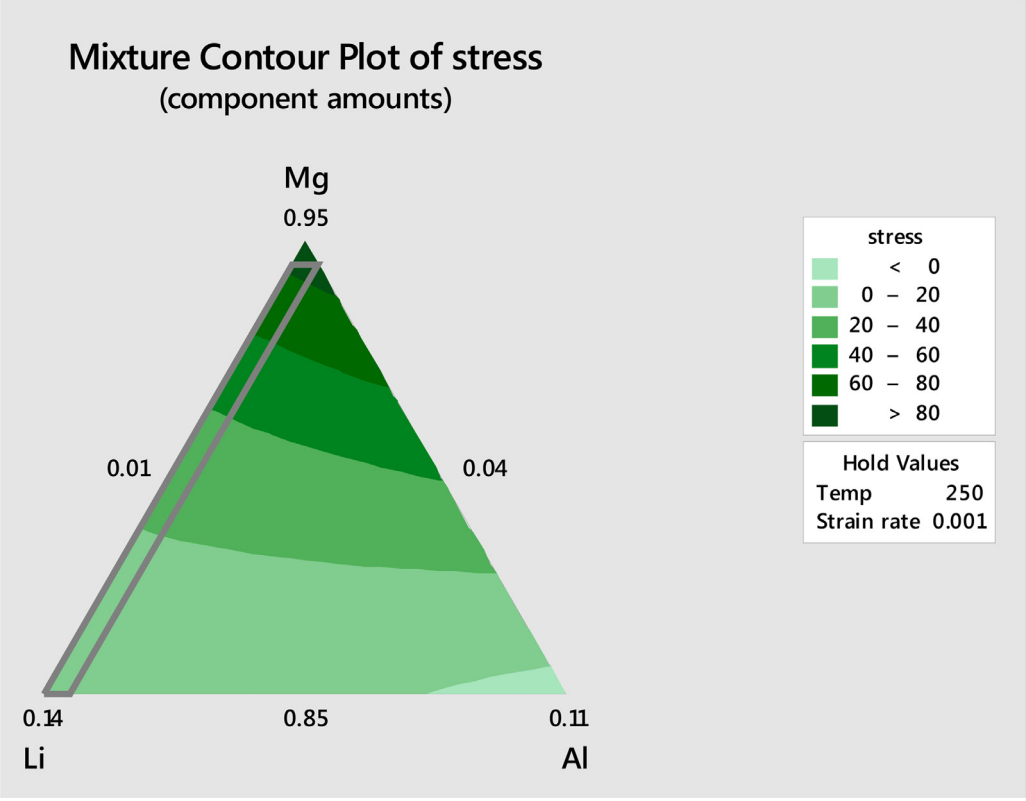

Fig. 11. Contour plot for a response.

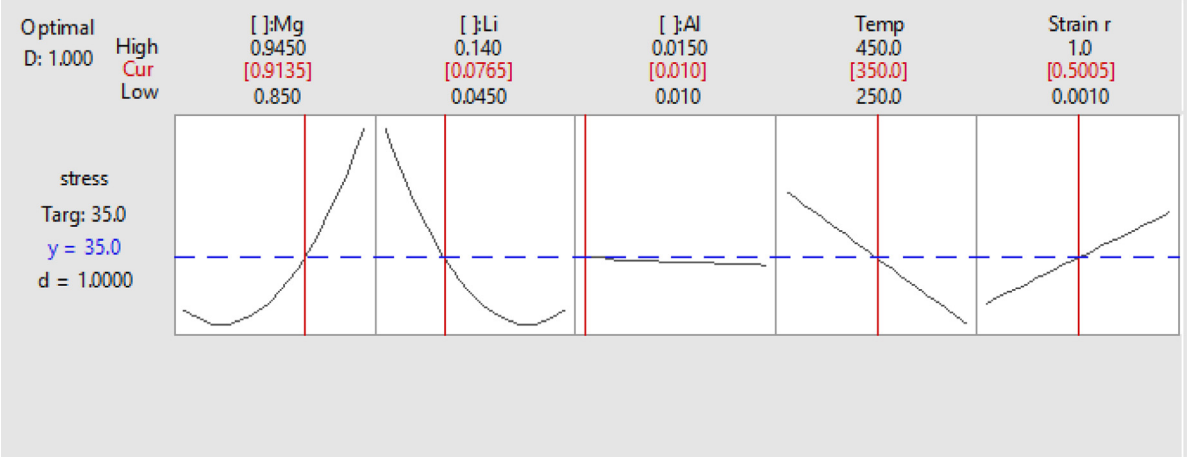

Fig. 12. Data optimization chart.

shows three components at a time while holding process variables at a constant level. Changing the holding levels, the response surface changes as well. The fitted responses are in the design space. And peak value of stress showed up when Mg percentage is high.

6.8. Contour plot

In the contour plot, Fig. 10, dark green region explicitly shows higher stress level when Mg is high in the proportion. Lighter green region demonstrates negative stress. Thus, it is considered an impossible region. In between these two extremes, the individual contours have divided the stress bands from 0–20 MPa, 20–40 MPa, 40–60 MPa, and 60–80 MPa. If the design demands an optimized stress of 35 MPa, the middle portion of design space should be chosen where the stress is in between 20–40 MPa.

7. Data optimization

Our target is to optimize the stress level (20 MPa, 25 MPa, 30 MPa, and 35 MPa). Some stress values have been randomly

selected to find the optimum condition. Upon some trial and error attempts in the Minitab 18, the 35-MPa stress is identified as the optimum condition. In Fig. 11, the blue dotted line demonstrates the optimized value of stress while the red solid lines show the factors and process variables current setting to get the optimized result. Finally, the optimum condition is composed of 91.35 wt% Mg, 7.65 wt% Li, 1wt%Al alloy when deformation temperature is 350 °C and 0.5/s strain rate. The results from this analysis fulfill the goal of this study. Since from the experimental analysis results and literature review, it is found that Li proportion between 5.5 wt% to 12wt% creates an alloy of better properties. Among these, around 8 wt%Li in Mg possesses the most ideal condition [19]. In the Mg-7.65% Li alloy, both α phase and β phase exist in the alloy and Al stabilizes the phases. By minimizing the stress, a combination of the stronger α phase with a more ductile β phase results in a material with the high specific strength is achieved. Fig. 12

8. Observation

The main observation from this analysis is that the variance inflation factor is significantly high. This means that the predictors are correlated. It is assumed that multi-linearity exits. This makes the model quite unreliable. If two variables are strongly negatively correlated, this might give a high VIF. In this design the main formulation factors Mg and Li are negatively correlated with each other that might rise VIF.

9. Conclusion

This study aims at assessing the blend of three types of components Mg, Li and Al by designing an extreme vertices mixture design. The results show that the proportion of different ingredients is effective for different stress level. The results of the contour plot show that the formula for each performance level can make a variety of formulas on possible graph areas. Therefore, choosing the most appropriate formulas can be found using the response optimizer to make the decision. The mean target of 35 MPa provides the optimum combination of 91.35 wt% Mg, 7.65 wt% Li, 1 wt%Al including the temperature of 350 °C and strain rate of 0.5/s. From actual experiments, it is evident that this combination renders good strength and better ductility. This analysis is not only to optimize the stress level but also to observe the stress variation with changing factors to improve the material properties. Contribution from this work will help to develop a new type of alloys using extreme vertices mixture design. The benefits of this technique are to reduce the time and save experimental cost. For the further analysis, it is required to improve the factors dependency on each other. In that way, multi-linearity will be reduced.

Appendix

A1. Design matrix

After creating the mixture design for imposed conditions the stress values are added as response and the following table is formed:

StdOrder	RunOrder	PtType	Blocks	Mg	Li	Al	Temp	Strain rate	stress
46	1	−1	1	0.87375	0.1125	0.01375	450	0.001	18.5
95	2	−1	1	0.87375	0.1125	0.01375	450	1	144.2
71	3	−1	1	0.87375	0.1125	0.01375	250	1	36.5
78	4	1	1	0.945	0.045	0.01	450	1	70.3
25	5	−1	1	0.92125	0.065	0.01375	250	0.001	7.2
3	6	1	1	0.945	0.045	0.01	250	0.001	36.2
10	7	−1	1	0.87375	0.115	0.01125	250	0.001	12.5
29	8	1	1	0.945	0.04	0.015	450	0.001	37.3
27	9	1	1	0.85	0.135	0.015	450	0.001	48.5
65	10	1	1	0.85	0.135	0.015	250	1	15.3
86	11	−1	1	0.87375	0.1125	0.01375	450	1	56.2
49	12	−1	1	0.92125	0.065	0.01375	450	0.001	143.2
87	13	−1	1	0.92125	0.0675	0.01125	450	1	2.2
81	14	2	1	0.8975	0.0925	0.01	450	1	5.6
80	15	2	1	0.85	0.1375	0.0125	450	1	14.8
38	16	−1	1	0.92125	0.065	0.01375	450	0.001	48.3
55	17	2	1	0.85	0.1375	0.0125	250	1	62.1
42	18	1	1	0.945	0.04	0.015	450	0.001	38.1
18	19	−1	1	0.87375	0.115	0.01125	250	0.001	36.5
66	20	1	1	0.945	0.045	0.01	250	1	2.1
64	21	1	1	0.85	0.14	0.01	250	1	144.6
74	22	−1	1	0.92125	0.065	0.01375	250	1	76.9
22	23	−1	1	0.92125	0.0675	0.01125	250	0.001	6.3
88	24	−1	1	0.92125	0.065	0.01375	450	1	7.1
40	25	1	1	0.85	0.135	0.015	450	0.001	37.2

(*continued on next page*)

(*continued*)

StdOrder	RunOrder	PtType	Blocks	Mg	Li	Al	Temp	Strain rate	stress
44	26	−1	1	0.87375	0.115	0.01125	450	0.001	37.1
69	27	−1	1	0.87375	0.115	0.01125	250	1	72.6
23	28	−1	1	0.92125	0.0675	0.01125	250	0.001	48.1
53	29	1	1	0.945	0.045	0.01	250	1	2.5
72	30	−1	1	0.92125	0.0675	0.01125	250	1	61.9
14	31	1	1	0.85	0.14	0.01	250	0.001	22.3
6	32	2	1	0.8975	0.0925	0.01	250	0.001	12.6
41	33	1	1	0.945	0.045	0.01	450	0.001	47.9
59	34	0	1	0.8975	0.09	0.0125	250	1	9.5
47	35	−1	1	0.92125	0.0675	0.01125	450	0.001	1.7
43	36	−1	1	0.87375	0.115	0.01125	450	0.001	21.6
100	37	−1	1	0.92125	0.065	0.01375	450	1	1.9
17	38	1	1	0.945	0.04	0.015	250	0.001	14
37	39	−1	1	0.92125	0.0675	0.01125	450	0.001	143.2
36	40	−1	1	0.87375	0.1125	0.01375	450	0.001	71.2
2	41	1	1	0.85	0.135	0.015	250	0.001	2.6
58	42	2	1	0.8975	0.0875	0.015	250	1	1.9
32	43	2	1	0.945	0.0425	0.0125	450	0.001	38.1
35	44	−1	1	0.87375	0.115	0.01125	450	0.001	36.3
92	45	1	1	0.945	0.04	0.015	450	1	70.8
24	46	−1	1	0.92125	0.065	0.01375	250	0.001	13.2
54	47	1	1	0.945	0.04	0.015	250	1	11.9
15	48	1	1	0.85	0.135	0.015	250	0.001	13.9
91	49	1	1	0.945	0.045	0.01	450	1	72.2
45	50	−1	1	0.87375	0.1125	0.01375	450	0.001	22.5
73	51	−1	1	0.92125	0.0675	0.01125	250	1	17.6
28	52	1	1	0.945	0.045	0.01	450	0.001	12.6
70	53	−1	1	0.87375	0.1125	0.01375	250	1	2.7
26	54	1	1	0.85	0.14	0.01	450	0.001	5.3
4	55	1	1	0.945	0.04	0.015	250	0.001	56.3
77	56	1	1	0.85	0.135	0.015	450	1	55.8
8	57	2	1	0.8975	0.0875	0.015	250	0.001	78.6
11	58	−1	1	0.87375	0.1125	0.01375	250	0.001	13.3
93	59	−1	1	0.87375	0.115	0.01125	450	1	13.6
31	60	2	1	0.8975	0.0925	0.01	450	0.001	77.3
61	61	−1	1	0.87375	0.1125	0.01375	250	1	2.2
60	62	−1	1	0.87375	0.115	0.01125	250	1	56.3
98	63	−1	1	0.92125	0.0675	0.01125	450	1	7.6
62	64	−1	1	0.92125	0.0675	0.01125	250	1	44.5
30	65	2	1	0.85	0.1375	0.0125	450	0.001	12.4
89	66	1	1	0.85	0.14	0.01	450	1	18.4
90	67	1	1	0.85	0.135	0.015	450	1	23.2
99	68	−1	1	0.92125	0.065	0.01375	450	1	9.8
57	69	2	1	0.945	0.0425	0.0125	250	1	43.9
52	70	1	1	0.85	0.135	0.015	250	1	78.5
85	71	−1	1	0.87375	0.115	0.01125	450	1	1.8
21	72	−1	1	0.87375	0.1125	0.01375	250	0.001	35.6
84	73	0	1	0.8975	0.09	0.0125	450	1	17.3
7	74	2	1	0.945	0.0425	0.0125	250	0.001	145
67	75	1	1	0.945	0.04	0.015	250	1	44.6
63	76	−1	1	0.92125	0.065	0.01375	250	1	1.9
1	77	1	1	0.85	0.14	0.01	250	0.001	47.6
50	78	−1	1	0.92125	0.065	0.01375	450	0.001	18.1
48	79	−1	1	0.92125	0.0675	0.01125	450	0.001	45.1
12	80	−1	1	0.92125	0.0675	0.01125	250	0.001	13.4
33	81	2	1	0.8975	0.0875	0.015	450	0.001	22.2
96	82	−1	1	0.87375	0.1125	0.01375	450	1	14.5
94	83	−1	1	0.87375	0.115	0.01125	450	1	62.4
16	84	1	1	0.945	0.045	0.01	250	0.001	8.6
5	85	2	1	0.85	0.1375	0.0125	250	0.001	57.1
51	86	1	1	0.85	0.14	0.01	250	1	9.7
97	87	−1	1	0.92125	0.0675	0.01125	450	1	56.4

(*continued on next page*)

(*continued*)

StdOrder	RunOrder	PtType	Blocks	Mg	Li	Al	Temp	Strain rate	stress
34	88	0	1	0.8975	0.09	0.0125	450	0.001	8.3
75	89	−1	1	0.92125	0.065	0.01375	250	1	70.4
13	90	−1	1	0.92125	0.065	0.01375	250	0.001	13.3
56	91	2	1	0.8975	0.0925	0.01	250	1	76.2
82	92	2	1	0.945	0.0425	0.0125	450	1	14.2
79	93	1	1	0.945	0.04	0.015	450	1	13.3
76	94	1	1	0.85	0.14	0.01	450	1	38.3
83	95	2	1	0.8975	0.0875	0.015	450	1	18.5
68	96	−1	1	0.87375	0.115	0.01125	250	1	2.3
9	97	0	1	0.8975	0.09	0.0125	250	0.001	44.3
39	98	1	1	0.85	0.14	0.01	450	0.001	1.8
19	99	−1	1	0.87375	0.115	0.01125	250	0.001	2.1
20	100	−1	1	0.87375	0.1125	0.01375	250	0.001	36.4

A2. Extreme vertices design

A2.1. Design summary

Components:	3	Design points:	100
Process variables:	2	Design degree:	2

Mixture total: 1.00000

A2.2. Number of boundaries for each dimension

Point type	1	2	0
Dimension	0	1	2
Number	4	4	1

A2.3. Number of design points for each type

Point type	1	2	3	0	−1
Distinct	16	16	0	4	16
Replicates	2	1	0	1	3
Total number	32	16	0	4	48

A2.4. Bounds of mixture components

	Amount		Proportion		Pseudo component	
Comp	Lower	Upper	Lower	Upper	Lower	Upper
A	0.8500	0.9450	0.8500	0.9450	0.0000	0.9500
B	0.0400	0.1400	0.0400	0.1400	0.0000	1.0000
C	0.0100	0.0150	0.0100	0.0150	0.0000	0.0500

* NOTE * Bounds were adjusted to accommodate specified constraints.

A2.5. Model summary

S	R-sq	R-sq(adj)	PRESS	R-sq(pred)
6.44977	97.07%	96.46%	5619.43	95.17%

A2.6. Estimated regression coefficients for stress (component proportions)

Term	Coef	SE Coef	*T*-Value	*P*-Value	VIF
Mg	152.1	44.2	*	*	3782.53
Li	7068	651	*	*	9448.73
Al	−141,790	290,405	*	*	32,335,601.92
Mg*Li	−9346	826	−11.32	0.000	11,640.33
Mg*Al	143,365	297,757	0.48	0.631	27,422,176.16
Li*Al	152,104	298,027	0.51	0.611	313,030.68
Mg*Temp	−142.1	44.2	−3.22	0.002	3782.53
Li*Temp	−3745	651	−5.75	0.000	9448.73
Al*Temp	−285,277	290,405	−0.98	0.329	32,335,601.92
Mg*Li*Temp	4940	826	5.98	0.000	11,640.33
Mg*Al*Temp	293,641	297,757	0.99	0.327	27,422,176.16
Li*Al*Temp	289,261	298,027	0.97	0.335	313,030.68
Mg*Strain rate	127.5	44.2	2.89	0.005	3782.53
Li*Strain rate	2868	651	4.41	0.000	9448.73
Al*Strain rate	440,328	290,405	1.52	0.133	32,335,601.92
Mg*Li*Strain rate	−3578	826	−4.33	0.000	11,640.33
Mg*Al*Strain rate	−452,174	297,757	−1.52	0.133	27,422,176.16
Li*Al*Strain rate	−449,589	298,027	−1.51	0.135	313,030.68

Coefficients are calculated for coded process variables.

A2.7. Model summary

S	R-sq	R-sq(adj)	PRESS	R-sq(pred)
6.52412	96.71%	96.38%	4800.77	95.88%

A2.8. Analysis of variance for stress (component proportions)

Source	DF	Seq SS	Adj SS	Adj MS	*F*-Value	*P*-Value
Regression	9	112,608	112,608	12,512.0	293.96	0.000
Component Only						
Linear	2	31,940	5930	2965.1	69.66	0.000
Quadratic	1	6746	6746	6745.7	158.48	0.000
Mg*Li	1	6746	6746	6745.7	158.48	0.000
Component * Temp						
Linear	2	47,240	30,504	15,251.9	358.33	0.000
Mg*Temp	1	35,989	10,739	10,738.9	252.30	0.000
Li*Temp	1	11,251	1881	1881.0	44.19	0.000
Quadratic	1	2167	2167	2167.3	50.92	0.000
Mg*Li*Temp	1	2167	2167	2167.3	50.92	0.000
Component * Strain rate						
Linear	2	23,144	8828	4414.2	103.71	0.000
Mg*Strain rate	1	21,984	4343	4342.7	102.03	0.000
Li*Strain rate	1	1161	1295	1295.1	30.43	0.000
Quadratic	1	1370	1370	1370.4	32.20	0.000
Mg*Li*Strain rate	1	1370	1370	1370.4	32.20	0.000
Residual Error	90	3831	3831	42.6		
Lack-of-Fit	42	3810	3810	90.7	207.87	0.000
Pure Error	48	21	21	0.4		
Total	99	116,438				

References

[1] M.K. Kulekci, Int. J. Adv. Manuf. Technol. 39 (2008) 851865, doi:10.1007/s00170-007-1279.
[2] E. Aghion, B. Bronfin, Mater. Sci. Forum 350–351 (2000) 19–30.
[3] V.N. Timofeev, V.N. Serebryany, Y.A. Zaliznyak, Russ. Metall. (Metally) 2008 (2008) 266.
[4] Z. Zeng, J.-F. Nie, S.-W. Xu, C.H.J. Davies, N. Birbilis, Nat. Commun. 8 (2017) 972.
[5] Q. Liu, A. Roy, V.V. Silberschmidt, Mech. Mater. 113 (2017) 44–56.
[6] C.O. Muga, Z.W. Zhang, Adv. Mater. Sci. Eng. (2016), Article ID 1078187, 11 pages.
[7] P.C. Wang, C.C. Lin, T.Y. Huang, H.C. Lin, Y.H. Lee, M.T. Yeh, J.Y. Wang, Mater. Trans. 49 (2008) 913–917.
[8] C.-T. Chiang, S. Lee, C.-L. Chu, Trans. Nonferrous Metals Soc. China 20 (8) (2010) 1374–1379.
[9] G.S. Song, M. Staiger, M. Kral, Enhancement of the properties of Mg-Li alloys by small alloying additions, Magnesium Technology 2003, The Minerals, Metals & Materials Society, 2003, pp. 77–79. edited by Howard I. Kaplan TMS.
[10] M. Esmaily, J.E. Svensson, S. Fajardo, N. Birbilis, G.S. Frankel, S. Virtanen, R. Arrabal, S. Thomas, L.G. Johansson, Prog. Mater Sci. 89 (2017) 92–193.
[11] P.B. Singh, R.K. Sabat, S. Kumaran, S. Suwas, J. Mater. Eng. 27 (2) (2018) 864–874.
[12] G. Liu, W. Xie, G. Wei, Y. Yang, J. Liu, T. Xu, W. Xie, X. Peng, Materials 11 (3) (2018) 408.
[13] Z. Drozd, Z. Trojanová, S. Kúdela, J. Alloys Compd. 378 (1–2) (2004) 192–195.
[14] G.H. Park, J.T. Kim, H.J. Park, Y.S. Kim, H.J. Jeong, N. Lee, Y. Seo, et al., J. Alloys Compd. 680 (2016) 116–120.
[15] X.-M. Zhang, J.-M. Chen, Y.-l. Deng, Y. Xiao, H. Jiang, Chin. J. Nonferrous Metals 15 (12) (2005) 1925–1932.
[16] W. Wangkananon, C. Phuaksaman, T. Koobkokkruad, S. Natakankitkul, Eng. J. 22 (2018) 175–185.
[17] S. Richmire, K. Hall, M. Haghshenas, J. Magn. Alloys 6 (2018) 215–228.
[18] J.L. Glajch, J.J. Kirkland, K.M. Squire, J.M. Minor, J. Chromatogr. A 199 (1980) 57–79.
[19] http://support.minitab.com/en-us/minitab/18/.
[20] G. Wei, X. Peng, A. Hadadzadeh, Y. Mahmoodkhani, W. Xie, Y. Yang, M.A. Wells, Mech. Mater. 89 (2015) 241–253.
[21] Y.P. Li, E. Onodera, H. Matsumoto, A. Chiba, Metal. Mater. Trans. A 40 (2009) 982–990.
[22] G.H. Park, J.T. Kim, H.J. Park, Y.S. Kim, H.J. Jeong, N. Lee, Y. Seo, J. Alloys Compd. 680 (2016) 116–120.
[23] Z. Trojanová, P. Palček, P. Lukáč, Z. Drozd, Magnesium Alloys-Properties in Solid and Liquid States, InTech, 2014.
[24] Y. Tang, W. Jia, X. Liu, Q. Le, J. Cui, Mater. Sci. Eng.: A 689 (2017) 332–344.
[25] https://support.minitab.com.
[26] https://support.minitab.com.
[27] Y. Yan, W.-P. Deng, Z.-F. Gao, J. Zhu, Z.-J. Wang, X.-W. Li, Acta Metal. Sin. (Engl. Lett.) 29 (2) (2016) 163–172.
[28] G. Liu, W. Xie, G. Wei, Y. Yang, J. Liu, T. Xu, W. Xie, X. Peng, Materials 11 (3) (2018) 408.